

Transient thermal characterization of organic light-emitting diodes

Lianqiao Yang, Bin Wei and Jianhua Zhang

Key Laboratory of Advanced Display and System Applications, Ministry of Education, 149 Yanchang Road, Shanghai University, Shanghai 200072, People's Republic of China

E-mail: yanglianqiao@shu.edu.cn

Received 20 April 2012, in final form 28 June 2012

Published 6 August 2012

Online at stacks.iop.org/SST/27/105011

Abstract

In this paper, a novel measurement approach of junction temperature and thermal resistance of organic light-emitting diodes (OLEDs) is reported. Transient thermal measurement is utilized to carry out the thermal study of OLEDs. A linear relationship between forward voltage and junction temperature is obtained at the sensor current of $0.56 \mu\text{A}$ for each pixel. The effects of input current and cooling conditions on the junction temperature and thermal resistance are discussed. It is found that the optical performance is greatly affected by the junction temperature. The average junction temperature of the OLED panel with the current density of 0.014 A cm^{-2} is 64.5°C , while there exists a temperature difference of 14.5°C and 43.5°C with the center case and ambient temperature. In contrast to the natural cooling condition, a much smaller junction temperature rise and thermal resistance are obtained under the forced cooling condition. The thermal resistance from junction to ambient has an inverse relationship with input power under both natural and forced cooling conditions.

(Some figures may appear in colour only in the online journal)

1. Introduction

Recently, organic light-emitting diodes (OLEDs) have attracted more and more interest due to the huge potential market and the many advantages of OLEDs [1]. Rapid developments in the electrical and optical performance of OLEDs have been obtained and the reliability problems have been solved to a certain level by the advanced packaging method [2, 3]. For the OLEDs, overheat not only directly accelerates the degradation of the organic function materials, but also may lead to crack or delamination because of the thermal gradient and mismatch of the thermal expansion coefficient for different packaging materials of OLEDs. Thermal management will be a more critical issue in the package and module of OLEDs with increasing power capability. Researchers have demonstrated the importance of thermal management for OLED reliability [4]. Tsuji [5] and Seungjun [6] measured the thermal performance by Raman scattering and infra-red method respectively. However, the measured temperature map reflected the glass substrate/cover rather than junction temperature, while a thermal gradient is expected to exist since materials with low thermal conductivity such as glass are usually used as substrate and cover. The

numerical simulation approach has also been used in the thermal analysis of the OLED array [7–9]. An electrical test method offers an indirect but accurate measurement approach for packaged device. Thermal transient measurements have been used for the qualification of the thermal behavior of semiconductor devices for more than 20 years [10].

In this paper, the junction temperature and thermal resistance of OLED panel are investigated *in situ* by the transient thermal measurement method for the first time. The thermal and optical performances of the OLED at various working conditions are studied and analyzed. The junction temperature is compared with the surface temperature and is related to optical efficacy.

2. Experimental process

The investigated OLED package is composed of glass substrate, anode, organic layers, cathode, and glass cover as shown in figure 1. The circle dot in the case surface center indicates the location for the case temperature measurement by thermocouple. The dotted rectangle indicates the junction temperature measurement by the electrical test method. The

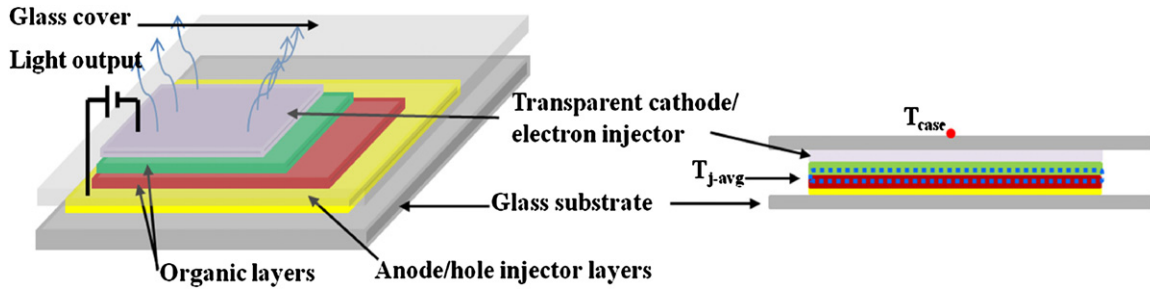


Figure 1. Schematic diagram of OLED sample and measurement location of thermocouple and electrical test measurement.

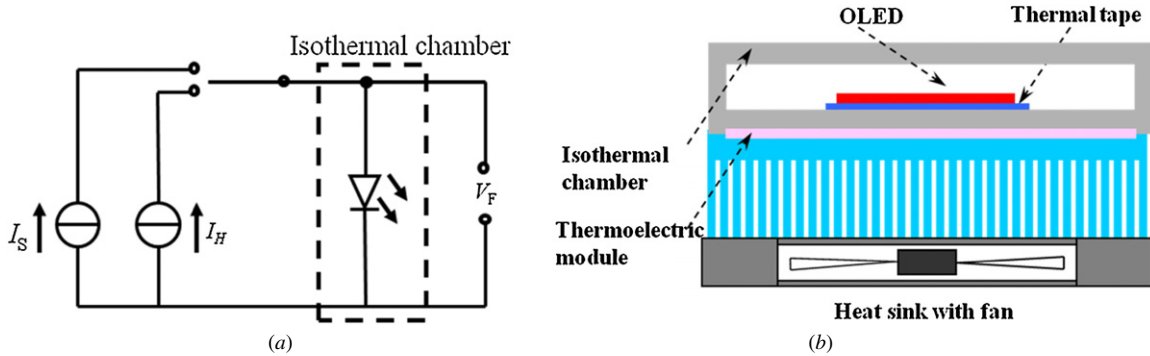


Figure 2. Schematic setup for (a) electrical test method (I_S and I_H are the sensor and heating current, V_F is the forward voltage) (b) thermostat.

investigated OLED panel has 1800 pixels with a dimension of 36*24 mm. All the pixels are connected in parallel. Due to the low thermal conductivity of glass and organic layers, the junction temperature is expected to be higher than the case temperature.

The Electronic Industries Association EIA/JEDEC 51-1 specification described the forward voltage (V_F)-based junction temperature (T_j) measurement technique for diodes. The basic principle of the electrical test method is to use the diode junction’s inherent voltage/temperature dependence as the temperature sensitive parameter (TSP). The J - V characteristics of OLED in the turn-on stage can be described by the thermionic emission model [11]:

$$J = J_{st} \left[\exp \left(\frac{qV_F}{nKT} \right) - 1 \right] \quad (1)$$

where J and V_F are the forward current and voltage, J_{st} is the reverse saturation current, q is the elemental charge, k is Boltzmann’s constant, T is the absolute temperature and n is the ideality factor.

In this paper, a Transient Thermal Tester (T3Ster, Mentor Graphics Ltd) was used to investigate the thermal behavior of the OLEDs. The schematic diagram for the electrical test method is shown in figure 2(a). Two current levels are utilized in the electrical test method: a low-level sensor current (in the turn-on stage and with light emitted out) and a high-level heating current. For the OLED, the V_F versus temperature relationship is determined by driving the OLED with the sensor current and adjusting temperature. The resulting points are graphed and the relationship is reduced to a single slope factor called the K -factor:

$$K = \frac{\Delta V_F}{\Delta T_j} = \ln \left(\frac{J}{J_{st}} + 1 \right) nk/q. \quad (2)$$

The schematic setup for the thermostat is shown in figure 2(b). The thermostat is composed of an isothermal chamber, thermoelectric module and heat sink with fan. As part of the T3ster, the thermostat can realize heating and refrigeration with the resolution of 0.2 °C. During the K calibration and thermal measurement of the OLED under forced cooling conditions, the OLED panel is attached to the bottom surface of the isothermal chamber with thermal tape as the thermal interface material.

Thermal transient measurement was done in the following procedures. After the calibration of K factor driven by sensor current in thermostat, the device is put into the scheduled environment. The detailed procedure of transient thermal measurement is shown in figure 3(a) and voltage variation during the process is shown in figure 3(b). T3Ster captures the voltage transients real-timely (right after t_2 in figure 3(a)) and then converts the data to thermal transients by combining with the K factor.

$$T_j = T_x + \Delta T = T_x + \Delta V_F/K \quad (3)$$

where T_x is the reference temperature. The obtained transient thermal response is evaluated to derive the thermal characteristics. Based on the thermal R - C network and structure function theory, the heat path can be determined quantitatively. The differential structure function is defined as the derivative of the cumulative thermal capacitance with respect to the cumulative thermal resistance:

$$K(R_\Sigma) = \frac{dC_\Sigma}{dR_\Sigma} = \frac{cAdx}{dx/\lambda A} = c\lambda A^2 \quad (4)$$

where C and R are the thermal capacitance and thermal resistance, c is the specific heat, A is the cross section area and λ is thermal conductivity.

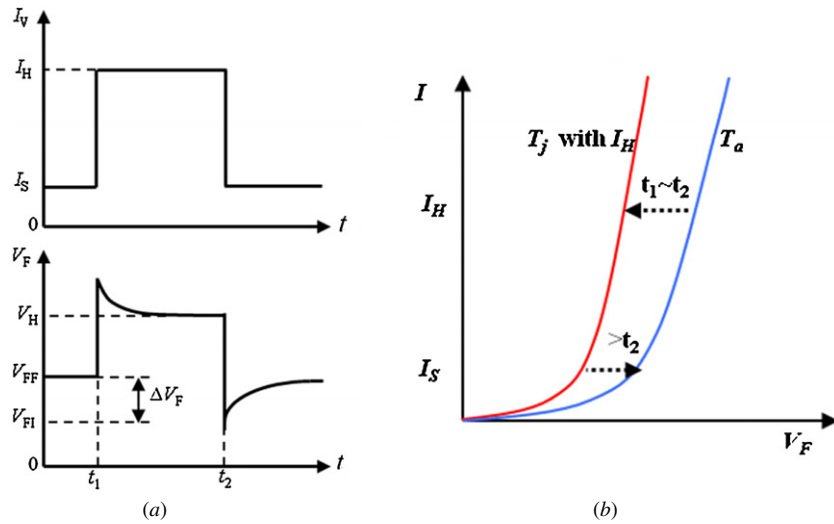


Figure 3. (a) Procedure of transient thermal measurement and (b) voltage variation during transient thermal measurement (I_S and I_H are the sensor and heating current, V_H is the forward voltage with the heating current, V_{FF} and V_{FI} is the final voltage and initial voltage at the sensor current after cutting off the heating current, ΔV_F is forward voltage change during the cooling process of the device).

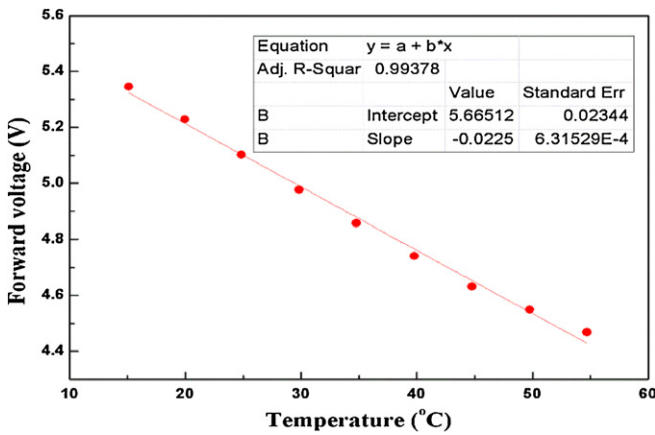


Figure 4. Calibrated K factor of OLED.

From equation (4), it can be seen that the peak in differential structure function means either a change in the material properties or a change in the geometry or both. Detailed information about the RC network can be seen in [10].

During the K factor calibration, the sensor current of 1 mA (0.56 μ A for each pixel) in the temperature range of 15–55 $^{\circ}$ C with an incremental temperature step of 5 $^{\circ}$ C is used. Transient measurement is started to record the cooling curve after driving the OLED samples for 10 min in a still air chamber in order to ensure that it reached thermal stabilization. The standard still air chamber according to JEDEC 51-2 is used for the condition of natural cooling.

The case temperature is measured by the physical contact method (K -type thermocouple). As shown in figure 1, the thermo-couple is attached to the center of the case surface.

3. Results and discussion

The calibrated K factor is shown in figure 4. A linear relationship between the forward voltage and junction

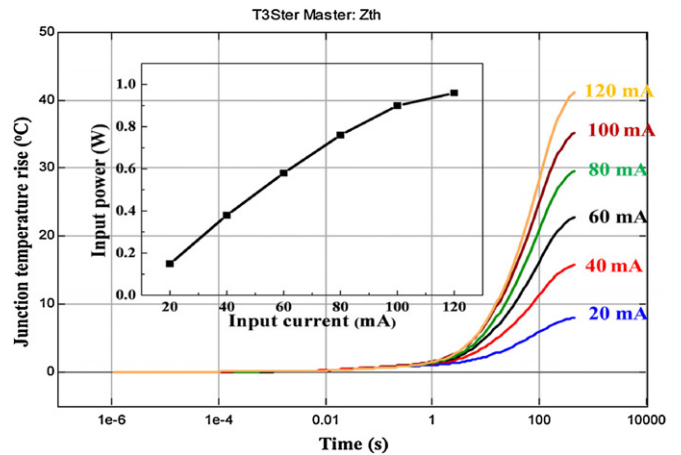


Figure 5. Junction temperature rise of OLED package with input current at a still air chamber; the inset graph is the input power variation with input current.

temperature is verified and the obtained K factor is $-0.023 \text{ mV } ^{\circ}\text{C}^{-1}$.

One thing to be noted is the measured result by the electrical test method is the average junction temperature of all the pixels [12]. The cooling curve variation of the OLED package with input current at room temperature of 23 $^{\circ}$ C is shown in figure 5.

It can be seen from figure 5 that the average junction temperature rise ($\Delta T_{j\text{-avg}}$) increased with the input current since the heating power increased as shown in the inset graph of figure 5. At a current density of $0.12/3.6*2.4 = 0.014 \text{ A cm}^{-2}$, the average junction temperature, which equals the sum of ambient temperature (23 $^{\circ}$ C) and average junction temperature rise (41.5 $^{\circ}$ C), has already reached 64.5 $^{\circ}$ C. It has been verified that the optical output and efficacy have an inverse variation trend with the working temperature [13]. Besides, a higher input current can lead to a higher junction temperature, which may cause a blue shift of the peak wavelength [14], variation

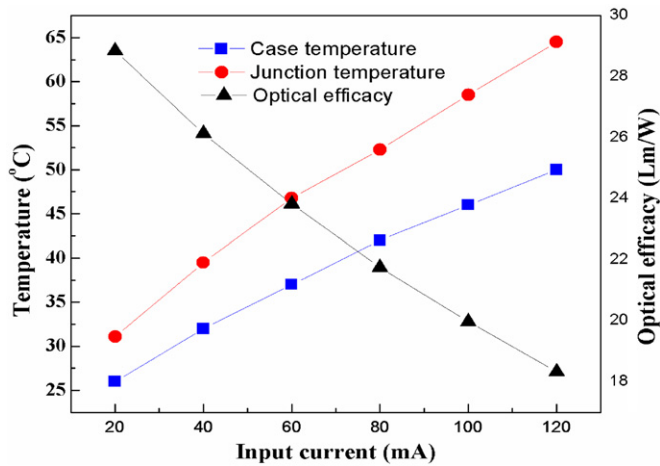


Figure 6. Optical efficacy, junction and center case temperature of the OLED package with input current at a still air chamber.

of carrier density [15], decompose of organic layers, crack or delamination [16].

The junction and case temperature and optical efficacy of the OLED as a function of input current are shown in figure 6. It can be seen that both junction and case temperature increase with the input current, but the thermal gradient between the junction and case temperature also increased from 5.1 °C to 14.5 °C when the input current increased from 20 mA to 120 mA. Thermal contact resistance, which depends on the scattering and radiation of phonon and electron at the interfaces among the composing layers, and the low thermal conductivity of organic and packaging materials are regarded as responsible for the large thermal gradient between the junction and case temperature. The optical efficacy shows an inverse trend with the temperature, and it decreased from 28.9 to 18.3 lm W⁻¹ when the input current increased from 20 to 120 mA. Therefore, figures 5 and 6 clearly show that the heat generated in OLED cannot be neglected and it is not appropriate to use case temperature to evaluate the thermal performance of OLED instead of the junction temperature.

The differential structure functions of OLED as a function of input current are shown in figure 7. The thermal resistance from junction to ambient is 56.2, 47.9, 41.9, 37.6, 34.0 and 30.7 K W⁻¹ at input current of 20, 40, 60, 80, 100 and 120 mA, respectively. Three reasons are regarded as responsible for the variation of measured thermal resistance from the junction to ambient. First of all, the dominant cooling mechanism for natural cooling is convection, which mainly depends on the heat transfer coefficient [17] as expressed:

$$h = 0.52C \left(\frac{\Delta T}{L} \right)^{0.25} \quad (5)$$

where C is a constant based on the geometry of the structure, L is the length of heat flow path and ΔT is the temperature difference between package surface and atmosphere temperature. The value of coefficient h increases with the input current and junction temperature, which leads to a decreased partial thermal resistance from case to ambient. Besides the convection effect, the thermal conductivity change

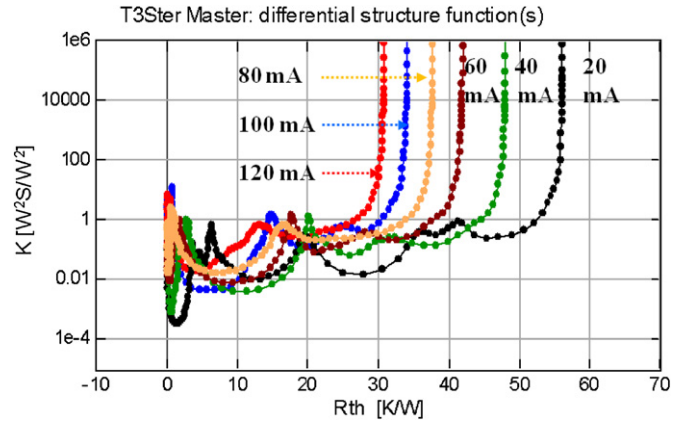


Figure 7. Structure function of OLED as a function of input current at a still air chamber.

of composing material is regarded as another reason for the decrease of thermal resistance with the input current. It is well known that the thermal resistance has a reverse relationship with the thermal conductivity for a certain package. The temperature dependence of various materials can be expressed as

$$\lambda = \lambda_0 \exp(\alpha_k(T - T_0)) \quad (6)$$

where λ is the thermal conductivity at T , λ_0 is the thermal conductivity at reference temperature T_0 , α_k is the temperature coefficient of λ , T is the temperature. α_k for glass, the dominant composing material of the OLED panel, is a positive value in the experimental temperature range [18], which can lead to the increase of thermal conductivity and decrease of thermal resistance with the operating temperature.

In addition to the above two factors, the optical effect is another reason affecting the thermal resistance evaluation. Accurately speaking, the thermal resistance for optical device should be defined as

$$R = (T_j - T_a)/P_{\text{heat}} = (T_j - T_a)/(P_e - P_{\text{opt}}) \quad (7)$$

where T_j and T_a are the junction and ambient temperature respectively, P_e and P_{opt} is the electrical and optical power of the OLED, P_{heat} is the heat generated by the OLED.

However, the measured thermal resistance (R_m) of OLED in this work is evaluated in the following way automatically by the equipment:

$$R_m = (T_j - T_a)/P_e. \quad (8)$$

Combining equations (7) and (8), the following equation can be obtained:

$$R_m = R(P_e - P_{\text{opt}})/P_e = R(1 - \eta_{\text{opt}}) \quad (9)$$

where η_{opt} is the optical efficacy. It is clear from equation (9) that the optical efficacy has a reverse relationship with the R_m in the case of R keeping as constant. The optical efficacy shows a declined trend with input current as talked before, which could make the measured thermal resistance exhibit increased trend.

In a word, the increase of convection coefficient (h) and thermal conductivity (λ) could make the thermal resistance decrease with the increase of input current. However,

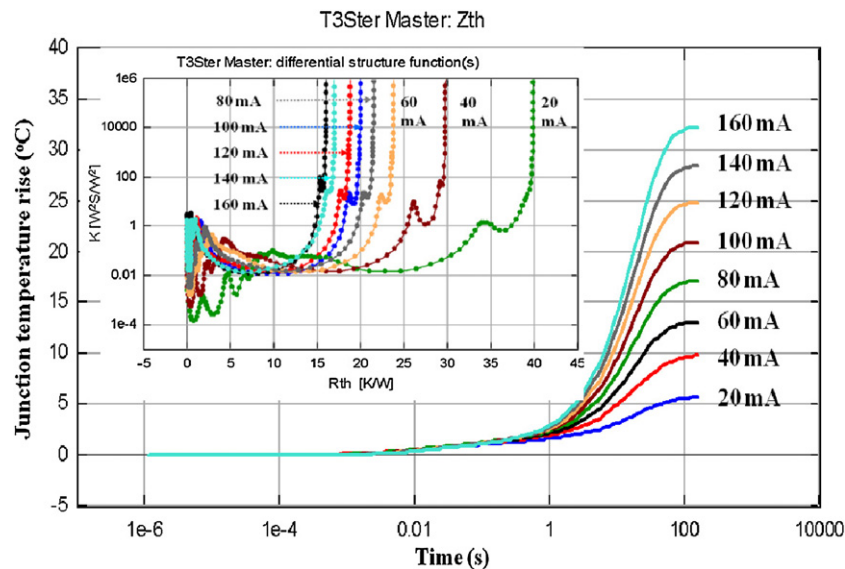


Figure 8. Junction temperature rise of OLED package as a function of input current at a fixed substrate temperature of 20 °C; the inset graph is the corresponding differential structure function.

the optical efficacy (η_{opt}) has a reverse effect on thermal resistance with increasing current. For the case of R_m versus input current under still air conditions, in variation of h and λ the dominant effect is used during the counterbalance of the three reasons.

The cooling curve of OLED as function of input current at fixed substrate temperature of 20 °C is shown in figure 8, and the inset graph is the corresponding differential structure function. Comparing the results from figures 7 and 8, it can be seen that the thermal resistance variation trends are the same for natural and forced cooling conditions. However, the junction temperature and thermal resistance under natural cooling conditions are much greater than those under forced cooling conditions at the same input current. At the same input current of 120 mA, the thermal gradient between the junction and ambient decreased from 41.5 °C to 24.9 °C; the thermal resistance is 30.7 K W⁻¹ and 18.7 K W⁻¹ for natural cooling and forced cooling, respectively. Effective thermal management can greatly reduce the junction temperature and increase the maximum input current and ensure the reliability [6].

Comparing figures 5 and 8, it can be obtained that all thermal responses start to grow at basically the same time, about 0.01 s. The thermal time constant, which depends on the geometric structure, thermal conductivity, specific heat and density of composing parts, directly decides the real time response of the device. Devices working under a pulse driven condition can take full advantage of the big thermal time constant to slow down the heating speed of the junction temperature. For the devices working under dc conditions, the saturated junction temperature depends only on the thermal resistance, but has no relationship with the time constant.

4. Conclusions

In this paper, we have reported an accurate thermal evaluation method of OLED packages by transient thermal measurement.

The average junction temperature and thermal resistance are determined under various working conditions. It is concluded that both junction and case temperature increase significantly with input current, and the thermal gradient between them becomes bigger with increasing input current. In contrast to the natural cooling condition, a much smaller junction temperature rise and thermal resistance are obtained under the forced cooling condition. The results provide strong motivation to further investigation of accurate junction temperature measurement of OLED packages in various structures and working conditions.

Acknowledgments

This work was financially supported by the Science and Technology Committee of Shanghai under the grant no 10ZR1412000 and SRF for ROCS, SEM.

References

- [1] Tang C W 1986 Two-layer organic photovoltaic cell *Appl. Phys. Lett.* **48** 183–5
- [2] Sun S C, Takeshi F, Cao J, Zhu W Q, Jiang X Y, Zhang Z L and Wei B 2009 High luminance microcavity organic light-emitting diodes *J. Optoelectron. Laser* **20** 609–11 http://en.cnki.com.cn/Article_en/CJFDTOTAL-GDZJ200905012.htm
- [3] Wang J, Wei B and Zhang J 2008 Fabricating an organic complementary inverter by integrating two transistors on a single substrate *Semicond. Sci. Technol.* **23** 055003
- [4] Vamvounis G, Aziz H, Hu N-X and Popovic Z D 2004 Temperature dependence of operational stability of organic light emitting diodes based on mixed emitter layers *Synth. Met.* **143** 69–73
- [5] Tsuji H, Oda A, Kido J, Sugiyama T and Furukawa Y 2008 Temperature measurements of organic light-emitting diodes by stokes and anti-stokes Raman scattering *Japan. J. Appl. Phys.* **47** 2171–3

- [6] Cheung S, Lee J-H, Jeong J, Kim J-J and Hong Y 2009 Substrate thermal conductivity effect on heat dissipation and lifetime improvement of organic light-emitting diodes *Appl. Phys. Lett.* **94** 253302
- [7] Slawinski M, Bertram D, Heuken M, Kalisch H and Vescan A 2011 Electrothermal characterization of large-area organic light-emitting diodes employing finite-element simulation *Org. Electron.* **12** 1399–405
- [8] Pohl L, Kollár E, Poppe A and Kohári Z 2011 Nonlinear electro-thermal modeling and field-simulation of OLEDs for lighting applications I: algorithmic fundamentals *Microelectron. J.* **43** 624–32
- [9] Poppe A, Pohl L, Kollár E, Kohári Zs, Lifka H and Tanase C Methodology for thermal and electrical characterization of large area OLEDs *Proc. of the 25th IEEE Semiconductor Thermal Measurement and Management Symp. (SEMI-THERM'09), (San Jose, USA 15–19 March 2009)* pp 38–44
- [10] Szabó P, Steffens O, Lenz M and Farkas G 2005 A methodology for the generation of dynamic compact models of packages and heat sinks from thermal transient measurements *IEEE Trans. Compon. Packag. Technol.* **28** 630–6
- [11] Brovelli F, Bernède J C, Marsillac S, Díaz F R, del Valle M A and Beaudouin C 2002 Study of the I – V characteristics of organic light emitting diodes based on thiophene vinyllic derivatives *J. Appl. Polym. Sci.* **86** 1128–37
- [12] Kim L and Shin M W 2007 Thermal resistance measurement of LED package with multichips *IEEE Trans. Compon. Packag. Technol.* **30** 632–6
- [13] Wantz G *et al* 2005 Temperature-dependent electroluminescence spectra of poly (phenylene-vinylene) derivatives-based polymer light-emitting diodes *J. Appl. Phys.* **97** 034505
- [14] Wantz G, Hirsch L and Dautel O J 2007 Temperature-dependent electroluminescence spectra of organic light emitting diodes based on thermally evaporated bis-imido-phenylene vinylene derivative *Appl. Phys. Lett.* **90** 162104
- [15] Kumar A *et al* 2005 Temperature and electric-field dependence of hole mobility in light-emitting diodes based on poly[2-methoxy-5-(2-ethylhexoxy)-1, 4-phenylene vinylene] *J. Appl. Phys.* **98** 024502
- [16] Gielen A W J, Barink M, Brand J V D and Mol A M B V 2009 The electro-thermal-mechanical performance of an OLED: a multi-physics model study *Proc. of 10th Conf. on Thermal, Mechanical and Multiphysics Simulation and Experiments in Micro-Electronics and Micro-Systems EuroSimE* pp 1–6
- [17] Hwang W J, Lee T H, Choi J H, Kim H K, Nam O H, Park Y J and Shin M W 2007 Thermal investigation of GaN-based laser diode package *IEEE Trans. Compon. Packag. Technol.* **30** 637–42
- [18] van der Tempel L, Melis G P and Brandsma T C 2000 Thermal conductivity of a glass: I. Measurement by the glass–metal contact *Glass Phys. Chem.* **26** 606–11